arXiv:physics/0504113v2 [physics.atom-ph] 9 Jun 2005

Spatially selective loading of an optical lattice by light–shift engineering using an auxiliary laser field

P. F. Griffin, K. J. Weatherill, S. G. MacLeod, R. M. Potvliege, and C. S. Adams
Department of Physics, University of Durham, Rochester Building, South Road, Durham DH1 3LE, England.
(Dated: February 2, 2008)

We report on a method of light–shift engineering where an auxiliary laser is used to tune the atomic transition frequency. The technique is used to selectively load a specific region of an optical lattice. The results are explained by calculating the differential light–shift of each hyperfine state. We conclude that the remarkable spatial selectivity of light–shift engineering using an auxiliary laser provides a powerful technique to prepare ultra-cold trapped atoms for experiments on quantum gases and quantum information processing.

PACS numbers: 39.25.+k, 31.10.+z, 32.60.+i, 03.67.-a, 03.75.-b, 42.62.-b

Optical dipole traps and optical lattices are finding an ever increasing range of applications in experiments on Bose-Einstein condensation (BEC) [1, 2, 3, 4], optical clocks [5], single–atom manipulation [6, 7], and quantum information processing (QIP) [8, 9]. In many applications, one is interested not only in the light–shift of the ground state, which determines the trap depth, but also the relative shift of a particular excited state. One has some control over this differential shift as the ground and excited states have different resonances, and the laser can be tuned to a 'magic' wavelength where the ground and excited state polarizabilities are the same [5, 7, 10]. However, using a 'magic' wavelength is not always appropriate either because one is no longer free to select the laser wavelength to minimize spontaneous emission, or because of the unavailability of suitable light sources.

In this paper, we report on a different method of light–shift engineering where a second laser field is used to control the excited state polarizability. One such method for controlling ground–state hyperfine polarizabilities is discussed in Ref. [11]. Light–shift engineering using an independent laser could have significant advantages over the use of a 'magic' wavelength for some applications, as it can be applied to specific regions of a trap. For example, we show how the technique can be used to selectively load a well defined region of an optical lattice. Specifically, we consider the case of loading ^{85}Rb atoms into a deep CO_2 laser lattice. A quasi-electrostatic lattice based on a CO_2 laser (wavelength 10.6 μm) is particulary attractive for trapping cold atoms or molecules as it combines low light scattering [12] with a lattice constant sufficiently large to allow single-site addressability [13]. We show that by focussing an additional laser (a Nd:YAG laser with wavelength 1.064 μm) on a specific region of the lattice we can selectively load only into sites in this region. This spatially selective loading is most effective when the cooling light is blue–detuned relative to the unperturbed atomic resonance. We explain the effect by calculating the differential light-shifts between the ground and excited states in the presence of two light fields. We show that only in the light–shift engineered region where the CO_2 and Nd:YAG laser beams overlap, is the differential shift negative allowing efficient laser cooling. In addition, we show that for red-detuned cooling light, light–shift engineering produces a significant enhancement in the number of atoms loaded into a deep optical trap.

The experimental set-up employed to demonstrate controlled loading by light–shift engineering is shown in Fig. 1. An octagonal vacuum chamber, fitted with home-made Zinc Selenide (ZnSe) UHV viewports [14] to accommodate the CO_2 laser beams, provides a background pressure of 1.2×10^{-10} Torr. A focussed Nd:YAG laser beam, with variable power, locally heats an alkali metal dispenser to provide a controllable source of thermal ^{85}Rb atoms [15]. A CO_2 laser beam, (propagating along the z–axis in Fig. 1) with power 45 W, is focussed to form a waist ($1/e^2$ radius) of 70 μm at the center of the chamber. The beam is collimated and retro–reflected to form a 1D optical lattice. The intensity of the CO_2 laser is controlled using an acousto-optic modulator (AOM). The intensity at the center of the lattice, $I_0 = 2.3 \times 10^6$ Wcm^{-2}, gives a ground state light–shift $U_0 = -\frac{1}{2}\alpha_0 I_0/(\epsilon_0 c) = h(-36$ MHz), where $\alpha_0 = 335\ a_0^3$ is the ground–state polarizability at 10.6 μm in atomic units. A Nd:YAG laser beam (propagating at +45° to the y axis in the xy plane) with power 7.8 W is focussed by a $f = 150$ mm lens to overlap with the CO_2 lattice in the trapping region. The Nd:YAG laser has a circular focus with a beam waist of 30 μm in the overlap region. This gives an intensity of $I_0 = 5.5 \times 10^5$ Wcm^{-2} leading to a ground state light–shift $U_0 = h(-18.6$ MHz) using our calculated value of $\alpha_0 = 722\ a_0^3$ at 1.064 μm. The CO_2 and Nd:YAG laser beams are linearly polarized along the x and z axes, respectively.

Loading of a CO_2 laser lattice is carried out as follows: The CO_2 and Nd:YAG laser beams are left on throughout the loading stage. We load a magneto-optical trap (MOT), centered on the dipole trap, with 2×10^7 ^{85}Rb atoms in typically 3 seconds. After the magnetic field is switched off, the cooling laser beam intensities are reduced from 55 mWcm^{-2} to 10 mWcm^{-2} and the detuning is increased to $\Delta = -8\Gamma$, where $\Gamma = 2\pi(6$ MHz) is the natural linewidth of the transition, to create an optical molasses. After 10 ms of molasses, the atom cloud has a typical temperature of 40 μK, measured by time–

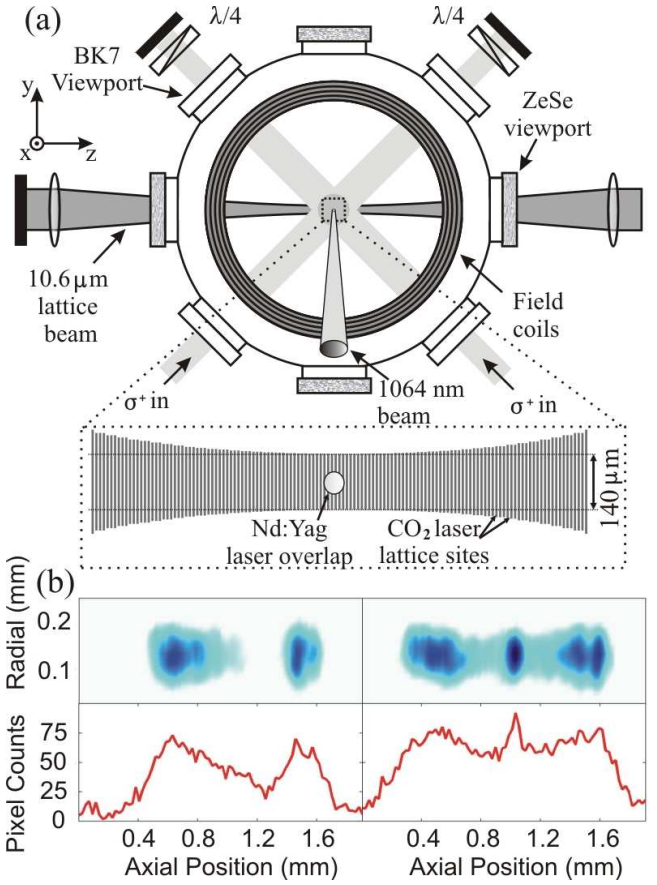

FIG. 1: (a) Experimental arrangement showing the intersection of the CO_2 and Nd:YAG laser beams. Inset: Schematic indicating the relative scales of the CO_2 and Nd:YAG spot sizes in the interaction region. (b) Images and line profiles without (left) and with (right) the Nd:YAG laser. The molasses detuning (-50 MHz) is chosen to optimize the total number of atoms rather than the number in the overlap region. The viewing direction is approximately perpendicular to both the CO_2 and Nd:YAG laser propagation directions.

shift between the ground and excited states away from the focus. We also see that the loading is greatly enhanced in the region where the Nd:YAG laser intersects the CO_2 laser lattice.

Remarkably, if we detune the cooling light slightly to the blue of the unperturbed atomic resonance such that neither the CO_2 nor the Nd:YAG laser beams alone trap any atoms, then we still observe that the region where the two beams intersect is efficiently loaded, see Fig. 2(b). This spatial selectivity provides a very clear demonstration of the power of light–shift engineering using an auxiliary laser field. In addition, it demonstrates that the enhanced loaded observed in Fig. 1 and Fig. 2(a) cannot be explained by a 'dimple' effect [19], where atoms from the wings of a trap rethermalise in the deeper overlap region [20].

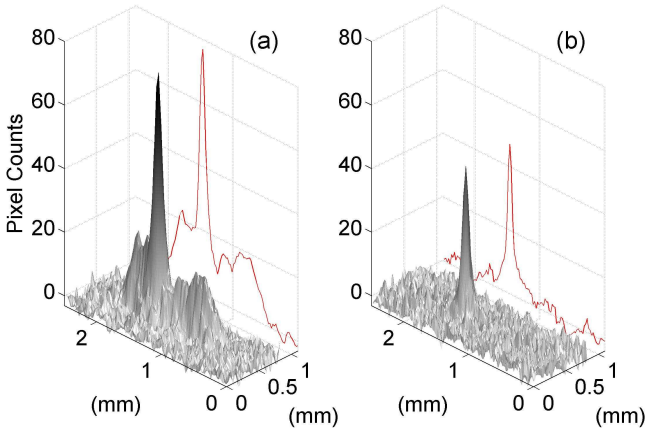

FIG. 2: A surface plot of the column density for cooling laser detunings (a) $\Delta = 2\pi(-20$ MHz) and (b) $\Delta = 2\pi(+2$ MHz). The on–axis density is shown on the back plane. For blue–detuning (b) only the light–shift engineered region, where the CO_2 and Nd:YAG laser beams overlap, is loaded.

of–flight. During the molasses phase the hyperfine repumping laser intensity is lowered from 6 mWcm^{-2} to 200 μWcm^{-2} and then switched off completely with a shutter for the final 5 ms such that atoms are pumped in the lower hyperfine state [16]. After the molasses phase, the cooling light and the Nd:YAG laser are extinguished for a few hundred milliseconds, then the CO_2 laser is turned off and the MOT beams (tuned to resonance) are turned back on to image the cloud. A CCD camera collects the fluorescence to give a spatial profile of the trapped atoms. A typical atom distribution viewed approximately perpendicular to the CO_2 and Nd:YAG beam axes is shown in Fig. 1(b). One sees that the CO_2 lattice loads efficiently out in the wings where the trap depth is smaller. This effect has been widely observed in experiments on far-off resonance optical dipole traps [13, 17, 18] and arises due to the smaller differential light–

Finally, we should add that the enhanced loading observed in the overlap region cannot be explained simply by the fact that the trap is deeper in this region. To demonstrate this we have reduced the CO_2 laser power by a factor of four such that the depth in the combined CO_2 plus Nd:YAG trap is less than a CO_2 lattice alone at full power. Typical column densities are shown in Fig. 3. We see that the density in the combined trap is still significantly higher than for a deeper CO_2 lattice.

To explain the spatially selective loading for blue–detuned cooling light, we have calculated the polarizability of the $5s$ ground and $5p$ excited states as a function of wavelength. The details of the calculation will be explained elsewhere [21]. Briefly, the scalar polarizability α_0 is the average of the dipole polarizabilities α_{xx}, α_{yy} and α_{zz} for an atom exposed to a laser field polarized, respectively, in the x, y, and z-directions: $\alpha_0 = (\alpha_{xx} + \alpha_{yy} + \alpha_{zz})/3$. The scalar polarizability is

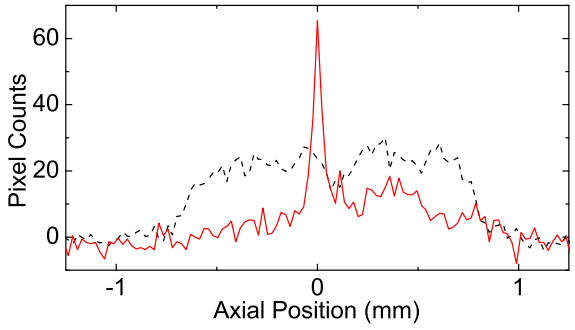

FIG. 3: Column density for a CO_2 laser lattice without the Nd:YAG laser (dashed line), and for a shallower CO_2 laser lattice with the Nd:YAG laser (solid line). The overall ground state light–shift in the overlap region of the shallow combined trap (-27 MHz) is less than the maximum light-shift for the CO_2 laser lattice alone (-36 MHz), but loading into the combined trap is still significantly more efficient. Both profiles are for a molasses detuning of -20 MHz.

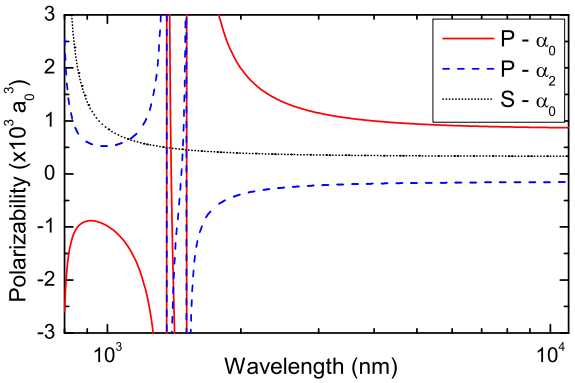

FIG. 4: Calculated polarizabilities of the $5s$ and $5p$ states of Rb. For the p state we show the scalar and tensor polarizabilities, $\alpha_0 = (\alpha_{xx} + \alpha_{yy} + \alpha_{zz})/3$ and $\alpha_2 = (\alpha_{xx} - \alpha_{zz})/3$, respectively. For the s state, $\alpha_0 = \alpha_{xx} = \alpha_{yy} = \alpha_{zz}$.

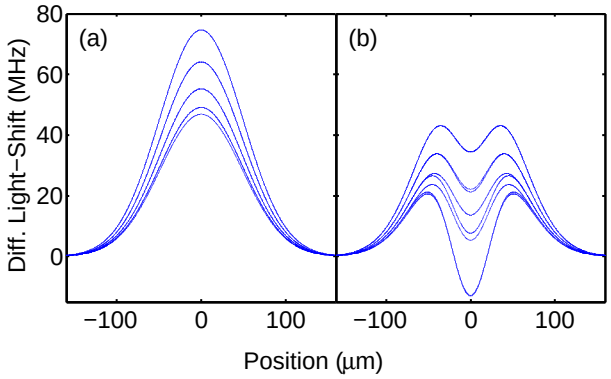

FIG. 5: The differential light–shifts as a function of position along an axis perpendicular to both the CO_2 and Nd:YAG laser propagation directions. The differential light–shift corresponds to the additional detuning of the cooling laser seen by ground–state atoms. It is equal to the light–shifts of the $m_F = -4, \ldots, +4$ magnetic sub-levels of the $5p^2P_{3/2}(F = 4)$ minus that of the ground state state in ^{85}Rb for atoms in (a) the CO_2 laser lattice only, and (b) in the combined CO_2 plus Nd:YAG trap.

the same for all m-components of the $5p$ state. In addition, there is a tensor polarizabilty $\alpha_2 = (\alpha_{xx} - \alpha_{zz})/3$ which lifts the degeneracy of different m-states. In order to obtain these quantities, we represent the interaction of the valence electron with the core by the model potential proposed by Klapisch [22]. The polarizabilities are calculated by the implicit summation method [23]. Thus α_{xx} (and similarly for α_{yy} and α_{zz}) is obtained as $\alpha_{xx} = -e(\langle 0|x|1\rangle + \langle 0|x|-1\rangle)/\mathcal{F}$, where $|0\rangle$ represents the state vector of the unperturbed $5s$, or $5p_{-1,0,1}$ states, and $|\pm 1\rangle$ are such that

$$(E_0 \pm \hbar\omega - H_0)|\pm 1\rangle = e\mathcal{F}x|0\rangle. \qquad (1)$$

Here H_0 is the Hamiltonian of the field-free model atom and E_0 is the eigenenergy of the unperturbed state, i.e. $H_0|0\rangle = E_0|0\rangle$, and $\mathcal{F}$ is an arbitrary electric field. These equations are solved in position space by expanding the wave functions on a discrete basis of radial Sturmian functions and spherical harmonics [24]. In the zero-frequency limit, the resulting values of $\alpha_0[5s]$, $\alpha_0[5p]$ and $\alpha_2[5p]$ converge towards $333a_0^3$, $854a_0^3$, and $-151a_0^3$, respectively, in satisfactory agreement with previous experimental and theoretical work [25]. The dynamic polarizabilities as functions of wavelength are shown in Fig. 4. We find that $\alpha_0 = 722a_0^3$ at 1.064 μm, which agrees well with experiment and other theoretical work [26, 27, 28].

For our purposes the most important result of Fig. 4 is that the polarizabilities of the $5s$ state at the CO_2 laser wavelength ($\lambda = 10.6$ μm) and the Nd:YAG wavelength ($\lambda = 1.064$ μm) have the same sign, whereas the polarizabilities of the $5p$ state have opposite signs. It follows that one can use a combination of CO_2 and Nd:YAG lasers to tune the differential light–shift between the $5s$ and $5p$ states through zero. To calculate the light–shift experienced by atoms in the combined CO_2 plus Nd:YAG trap we calculate the eigenvalues of the matrix [29, 30]

$$\mathsf{U} = \mathsf{U}_0 - \frac{1}{2\epsilon_0 c}\sum_{i=1,2}(\alpha_0^i \mathbb{1} + \alpha_2^i \mathsf{Q}^i)I_i\ , \qquad (2)$$

where U_0 is a diagonal matrix with components corresponding to the hyperfine splitting, the index i denotes the CO_2 and Nd:YAG lasers, and Q^i is a matrix with components $\langle F, m_F|Q_\mu|F', m_F'\rangle$ with $Q_\mu = [3\hat{J}_\mu^2 - J(J+1)]/J(2J-1)$ and J_μ being the electronic angular momentum operator in the direction of laser field i. The differential light–shift between the ground state and the $5p^2P_{3/2}(F = 4)$ state for the CO_2 laser alone is shown in Fig. 5(a). As a single laser beam splits the states according to the magnitude of m_F, there are five

curves corresponding to $|m_F| = 0, \ldots, 4$. We see that all the levels are far blue-detuned (positive differential shift) at the centre of the lattice, making laser cooling ineffective unless the cooling light is detuning to the red by an amount larger than the differential light–shift. Adding the Nd:YAG laser produces the shifts shown in Fig. 5(b). The Nd:YAG laser lifts the degeneracy between the $\pm m_F$ components, although two pairs of states remain close to degenerate. More importantly, one pair of states is pulled down into the region of negative differential shift. This allows efficient laser cooling in the center of the overlap region, even when the cooling light is slightly blue–detuned relative to the unperturbed resonance frequency. Note that, efficient loading for blue–detuning can only be explained if one includes the tensor polarizability term α_2. Although α_2 is smaller than the scalar polarizability (by a factor of 4 or 5), it dramatically alters whether states see the cooling light as red or blue detuned and therefore completely determines whether the trap is loaded or not.

As light–shift engineering allows laser cooling to work as efficiently as in free space one might expect to load atoms at lower temperature than in conventional loading schemes. To address this issue we need to increase the sensitivity and the resolution of our imaging system to allow accurate density and temperature measurements. This will be the focus of future work.

To conclude, we have shown how light-shift engineering using an auxiliary laser field can be used to implement spatially selective loading of deep far-off resonance optical lattices. We have performed theoretical calculations of the atomic polarizabilities and have shown that the addition of a second laser field induces a splitting of the excited state which is crucial in determining the efficiency of loading into the combined trap. The technique could be applied to load a single-site in 3D CO_2 lattice, with the interesting prospect of BEC in the limit of high trap frequency. In addition one could adapt the technique to perform patterned loading of optical lattices [31] for applications in QIP experiments.

We thank E. Riis, I. G. Hughes, and S. L. Cornish for stimulating discussions, M. J. Pritchard for experimental assistance and EPSRC for financial support.

[1] M. Barrett, J. Sauer, and M. S. Chapman, Phys. Rev. Lett. **87**, 010404 (2001).
[2] T. Weber, J. Herbig, M. Mark, H.-C. Nägerl, and R. Grimm, Science **299** 232 (2003).
[3] Y. Takasu, K. Maki, K. Komori, T. Takano, K. Honda, M. Kumakura, T. Yabuzaki, and Y. Takahashi, Phys. Rev. Lett. **91**, 040404 (2003).
[4] T. Kinoshita, T. Wenger, and D. S. Weiss, Phys. Rev. A **71**, 011602(R) (2005).
[5] H. Katori, T. Ido, amd M. K. Gonokami, J. Phys. Soc. Jap. **68**, 2479 (1999); H. Katori, M. Takamoto, V. G. Pal'chikov, and V. D. Ovsiannikov, Phys. Rev. Lett. **91**, 173005 (2003).
[6] N. Schlosser, G. Reymond, P. Grangier, Phys. Rev. Lett. **89**, 023005 (2002).
[7] J. McKeever, J. R. Buck, A. D. Boozer, A. Kuzmich, H.-C. Nägerl, D. M. Stamper-Kurn, and H. J. Kimble, Phys. Rev. Lett. **90**, 133602 (2003).
[8] O. Mandel, M. Greiner, A. Widera, T. Rom, T. W. Hänsch, and I. Bloch, Nature **425**, 937 (2003).
[9] D. Schrader, I. Dotsenko, M. Khudaverdyan, Y. Miroshnychenko, A. Rauschenbeutel, and D. Meschede, Phys. Rev. Lett. **93**, 150501 (2004).
[10] C. Degenhardt, H. Stoehr, U. Sterr, F. Riehle, and C. Lisdat, Phys. Rev. A. **70**, 023414 (2004).
[11] A. Kaplan, M. F. Andersen, and N. Davidson, Phys. Rev. A **66**, 045401 (2002)
[12] S. R. Granade, M. E. Gehm, K. M. OHara, and J. E. Thomas, Phys. Rev. Lett. **88**, 120405 (2002).
[13] R. Scheunemann, F. S. Cataliotti, T. W. Hänsch, and M. Weitz, J. Opt. B **2** 645 (2000).
[14] S. G. Cox, P. F. Griffin, C. S. Adams, D. DeMille, and E. Riis, Rev. Sci. Instrum. **74**, 3185 (2003).
[15] P. F. Griffin, K. J. Weatherill, and C. S. Adams, Rev. Sci. Instrum. submitted.
[16] C. S. Adams, H. J. Lee, N. Davidson, M. Kasevich, and S. Chu, Phys. Rev. Lett. **74**, 3577 (1995).
[17] S. J. M. Kuppens, K. L. Corwin, K. W. Miller, T. E. Chupp, and C. E. Wieman, Phys. Rev. A **62**, 013406 (2000).
[18] G. Cennini, G. Ritt, C. Geckeler and M. Weitz, Appl. Phys. B **77**, 773 (2003).
[19] D. M. Stamper-Kurn, H.-J. Miesner, A. P. Chikkatur, S. Inouye, J. Stenger, and W. Ketterle, Phys. Rev. Lett. **81** 2194 (1998); Z.-Y. Ma, C. J. Foot, and S. L. Cornish, J. Phys. B. **37** 3187 (2004).
[20] Y. Takasu, K. Honda, K. Komori, T. Kuwamoto, M. Kumakura, Y. Takahashi, and T. Yabuzaki, Phys. Rev. Lett. **90**, 023003 (2003).
[21] R. M. Potvliege and C. S. Adams, in preparation.
[22] M. Klapisch, C. R. Acad. Sci. Ser. B **265**, 914 (1967).
[23] A. Dalgarno and J. T. Lewis, Proc. R. Soc. A **233**, 70 (1955); C. Schwartz, Ann. Phys. (NY) **6**, 156 (1959).
[24] R. M. Potvliege, Comput. Phys. Commun. **114**, 42 (1998).
[25] M. S. Safronova, W. R. Johnson, and A. Derevianko, Phys. Rev. A **60**, 4476 (1999); S. Magnier and M. Aubert-Frécon, J. Quant. Spectrosc. Ra. **75**, 121 (2002); C. Zhu, A. Dalgarno, S. G. Porsev, and A. Derevianko, Phys. Rev. A **70**, 032722 (2004).
[26] M. S. Safronova, C. J. Williams, and C. W. Clark, Phys. Rev. A **69**, 022509 (2004).
[27] K. D. Bonin and M. A. Kadar-Kallen, Phys. Rev. A **47**, 944 (1993).
[28] M. Marinescu, H. R. Sadeghpour, and A. Dalgarno, Phys. Rev. A **49**, 5103 (1994).
[29] J. R. P. Angel and P. G. H. Sandars, Proc. Roy. Soc. A **305**, 125 (1968).
[30] R. W. Schmieder, Am. J. Phys. **40**, 297 (1973).
[31] S. Peil, J. V. Porto, B. L. Tolra, J. M. Obrecht, B. E. King, M. Subbotin, S. L. Rolston, and W. D. Phillips, Phys. Rev. A **67**, 051603(R) (2003).